ORIGINAL PAPER

Adaptive generalized function matrix projective lag synchronization of uncertain complex dynamical networks with different dimensions

Hao Dai · Gangquan Si · Yanbin Zhang

Abstract Generalized function matrix projective lag synchronization of uncertain complex dynamical networks with different dimension of nodes via adaptive control method is investigated in this paper. Based on Lyapunov stability theory, adaptive controller is obtained and unknown parameters of both the drive network and the response network are estimated by adaptive laws. In addition, the three-dimension chaotic system and the four-dimension hyperchaotic system, respectively, as the nodes of the drive and response network are analyzed in detail, and numerical simulation results are presented to illustrate the effectiveness of the theoretical results.

Keywords Complex dynamical network · Adaptive control · Generalized function matrix projective lag synchronization · Lyapunov stability theory

1 Introduction

Since the 1980s, as the rapid development of computer and information engineering technology, the human society has entered a "network era". In general, a complex network is a large set of interconnected nodes, in which a node is a fundamental unit with specific contents. The mathematical abstraction of a complex network is a graph G, comprising a set of N nodes (or vertices) connected by a set of M links (or edges), being k_i the degree (number of links) of node i. The node is used to represent the different individuals in real system, and the edge is used to indicate the relationships between different individuals. The nature of complex networks is the complexity, including complex topological structure, complex dynamical evolution, node diversity, connection diversity, and so on. Many real networks can be described by complex networks, which are shown to widely exist in various fields of real world, such as the Internet, the World Wide Web, biological networks, metabolic networks, transportation networks, phone call networks, communication networks, aviation networks, interpersonal relationship networks, electricity distribution networks, and so forth. The nodes and edges have different meanings in these different real networks. Recently, since the discovery of "small-world networks" [1] and "scale-free networks" [2], complex networks become a focus point of research which has attracted increasing attention from various fields of science and engineering.

Synchronization is a significant and interesting nonlinear phenomenon of nature, discovered at the beginning of the modern age of science by Huygens in 1673. Synchronization processes are ubiquitous in our

H. Dai · G. Si (✉) · Y. Zhang
State Key Laboratory of Electrical Insulation
and Power Equipment, School of Electrical Engineering,
Xi'an Jiaotong University, Xi'an, Shaanxi Province
710049, P.R. China
e-mail: sigangquan@mail.xjtu.edu.cn

lives, which play a very important role in many different contexts, such as synchronous communication, signal synchronization (for example, synchronization between video and audio signals), firefly bioluminescence synchronization in biology, geostationary satellite, synchronous motor, database synchronization and so forth. Pecora and Carroll [3] used the master stability function approach to determine the stability of the synchronous state in coupled systems. Recently, the synchronization of complex networks has been a focus in various fields of science and engineering, especially in field of control. The synchronization within one network is named "inner synchronization", which is concerned with the synchronization among the nodes with in a network. Different from the "inner synchronization", the synchronization between two or more complex networks regardless of synchronization of the inner network, which is called "outer synchronization", always does exist in our lives. In fact, there are a lot of research methods and synchronization ideas coming from the chaos synchronization. In [4], the authors studied chaotic synchronization and anti-synchronization for a novel class of multiple chaotic systems via a sliding mode control scheme. Impulsive control and synchronization of a new unified hyperchaotic system were investigated in [5]. Adaptive synchronization and lag synchronization of uncertain dynamical system was studied in [6]. In [7], the authors studied projective synchronization by using active control approach. These synchronization methods or ideas can be applied to the synchronization of complex network. In [8, 9], the authors studied synchronization in small-world dynamical networks and scale-free dynamical networks, respectively. Linear generalized synchronization between two complex networks was studied in [10]. The authors studied adaptive synchronization of two nonlinearly coupled complex dynamical networks with delayed coupling in [11]. Pinning synchronization of weighted complex networks was investigated in [12]. In [13], pinning adaptive controllers were designed to synchronize two general complex dynamical networks with non-delayed and delayed coupling. In [14], the authors studied synchronization between two different general complex dynamical networks with fractional-order chaos nodes. And then generalized projective synchronization and function projective synchronization for dynamical networks with non-identical nodes were investigated in [15, 16],

and impulsive synchronization of complex networks was investigated in [17]. In [18], the authors studied projective and lag synchronization between general complex networks. The synchronization was investigated in the above references is all outer synchronization, and this means that to study the dynamics between two coupled networks is necessary and important.

To the best of our knowledge, most of the existing papers discuss the synchronization between two complex networks with identical or non-identical nodes, and the dynamical equations of these network nodes have the same dimension [19–27]. However, in many real physics systems, the synchronization is carried out through the oscillators with different dimensions, especially the systems in biological science and social science. There exist many types of synchronization such as complete synchronization [28], anti-synchronization [29], phase synchronization [30], lag synchronization [31], projective synchronization [32] and so on. These types of synchronization are not suitable for unequal dimension system. For the complex dynamical systems with different dimensions, matrix synchronization is proposed in this paper. We use the matrix as a bridge, and achieve the synchronization between two different dimensional complex dynamical networks. The traditional model of the synchronization that a variable of response dynamical networks only corresponding to a variable of drive dynamical networks during the synchronization process is broken by the matrix synchronization. Therefore, the generalized function matrix projective lag synchronization (GFMPLS) between two different dimensional complex dynamical networks is investigated in this paper. GFMPLS includes projective synchronization (PS), lag synchronization (LS), function projective synchronization (FPS), matrix projective synchronization (MPS) and generalized function projective synchronization (GFPS), and it is a more general form of generalized synchronization. In addition, the complex dynamical networks not only have different dimension of network nodes but also unknown parameters.

This paper focuses on the adaptive generalized function matrix projective lag synchronization for uncertain complex dynamical network with unknown parameters and different dimensions of network nodes. Based on Lyapunov stability theory, an adaptive controller is obtained, and unknown parameters of both

the drive and the response networks are estimated by adaptive laws. In addition, the three-dimension chaotic system and the four-dimension hyperchaotic system, respectively, as the nodes of the drive and response networks are analyzed in detail, and numerical simulation results are presented to illustrate the effectiveness of the theoretical results.

The outline of the rest of the paper is organized as follows. Section 2 gives the network models and some useful preliminaries. In Sect. 3, by means of the adaptive control method, some sufficient synchronization criteria are derived to guarantee GFMPLS for uncertain complex dynamical networks with different dimensions of network nodes. Section 4 uses some representative examples to validate the effectiveness of the proposed approach. Finally, some concluding remarks are drawn in Sect. 5.

2 Network models and preliminaries

2.1 Network models

Some necessary mathematical notations that will be utilized throughout this paper are first introduced as follows. Let A^T (or x^T) be the transpose of the matrix A (or vector x). $\|x\|$ means the 2-norm of the vector x, and $\otimes$ denotes the Kronecker product of two matrices. $\lambda_{\max}(A)$ represents the maximum eigenvalue of a square matrix A.

In this paper, we consider a complex dynamic network consisting of N linearly coupled nodes with unknown parameters as the drive network, which is described by

$$
\dot{x}_i(t) = F_i\big(x_i(t)\big)\Phi_i + f_i\big(x_i(t)\big) + \sum_{j=1}^{N} c_{ij} P x_j(t),
$$
$$
i = 1, 2, \ldots, N, \tag{1}
$$

where $x_i = (x_{i1}, x_{i2}, \ldots, x_{in})^T \in R^n$ is the state vector of the ith node; $\Phi_i \in R^r$ is the unknown constant parameter vector; $F_i : R^n \to R^{n \times r}$ and $f_i : R^n \to R^n$ are the known continuous nonlinear function matrices. $P \in R^{n \times n}$ is an inner coupling matrix, which means two coupled nodes are linked through their ith state variables. $C = (c_{ij})_{N \times N} \in R^{N \times N}$ is the coupling configuration matrix representing the coupling strength and the topological structure of the network. The matrix C is defined as follows: if there exists a connection

from node j to node i $(i \neq j)$, then $c_{ij} \neq 0$; otherwise $c_{ij} = 0$. The diagonal elements of matrix C are defined by

$$
c_{ii} = - \sum_{j=1, j\neq i}^{N} c_{ij}, \quad i = 1, 2, \ldots, N.
$$

The response network with a nonlinear control scheme is given by

$$
\dot{y}_i(t) = G_i\big(y_i(t)\big)\Psi_i + g_i\big(y_i(t)\big)
$$
$$
+ \sum_{j=1}^{N} d_{ij} Q y_j(t) + u_i(t), \quad i = 1, 2, \ldots, N, \tag{2}
$$

where $y_i = (y_{i1}, y_{i2}, \ldots, y_{im})^T \in R^m$ is the state vector of the ith node; $\Psi_i \in R^s$ is the unknown constant parameter vector; $G_i : R^m \to R^{m \times s}$ and $g_i : R^m \to R^m$ are the known continuous nonlinear function matrices. $Q \in R^{m \times m}$ is also an inner coupling matrix and $D = (d_{ij})_{N \times N} \in R^{N \times N}$ is the coupling configuration matrix, which has the same meaning as that of matrix C. $u_i(t) \in R^m$ are the nonlinear adaptive controllers.

2.2 Preliminaries

The synchronization error signal for GFMPLS is defined as follows:

$$
e_i(t) = \begin{bmatrix} e_{i1}(t) \\ e_{i2}(t) \\ \vdots \\ e_{im}(t) \end{bmatrix}
$$
$$
= y_i(t) - M(t)x_i\big(t - \tau(t)\big)
$$
$$
= \begin{bmatrix} y_{i1}(t) \\ y_{i2}(t) \\ \vdots \\ y_{im}(t) \end{bmatrix} - M(t) \begin{bmatrix} x_{i1}(t - \tau(t)) \\ x_{i2}(t - \tau(t)) \\ \vdots \\ x_{in}(t - \tau(t)) \end{bmatrix},
$$
$$
i = 1, 2, \ldots, N, \tag{3}
$$

where $\tau(t) > 0$ is the time-varying delay, $M(t) = (m_{ij}(t)) \in R^{m \times n}$ is the time-varying scaling matrix, and the element in each row cannot be equal to zero at the same time.

If the element in a row is equal to zero at the same time, such that

$$e_{ij}(t) = y_{ij}(t) - \begin{bmatrix} 0 & 0 & \cdots & 0 \end{bmatrix} \begin{bmatrix} x_{i1}(t - \tau(t)) \\ x_{i2}(t - \tau(t)) \\ \vdots \\ x_{in}(t - \tau(t)) \end{bmatrix}$$

$$= y_{ij}(t), \tag{4}$$

then the network synchronization is meaningless.

Definition 1 Let $x_i(t - \tau(t))$ be the time delay state of the drive network (1), and $y_i(t)$ be the current state of the response network (2). Given the time-varying delay $\tau(t) > 0$, if there exist the time-varying scaling function matrix $M(t) = (m_{ij}(t)) \in R^{m \times n}$, and the element in each row cannot be equal to zero at the same time, such that

$$\lim_{t \to \infty} \left\| y_i(t) - M(t)x_i(t - \tau(t)) \right\| = 0,$$
$$i = 1, 2, \ldots, N, \tag{5}$$

then it is said that we achieve GFMPLS between networks (1) and (2).

Remark 1 If $m = n$ and the scaling functions matrix $M(t) = \text{diag}(k_1(t), k_2(t), \ldots, k_m(t))$, where $k_i(t)$ $(i = 1, 2, \ldots, m)$ is the function of the time t, then the drive and response networks would realize generalized function projective lag synchronization (GFPLS). If k_i $(i = 1, 2, \ldots, m)$ is the nonzero constants, then the GFPLS degenerates into generalized projective lag synchronization (GPLS). In particular, when the nonzero constant is chosen as 1, then the GPLS degenerates into the common lag synchronization (LS). In short, GFMPLS is a more general form that includes many kinds of synchronization as its special cases.

Assumption 1 The time-varying delay $\tau(t) > 0$ is a monotone increasing/decreasing continuous function, or $\tau(t) = \tau > 0$ is a constant. At the same time, the time-varying delay $\tau(t)$ is a bounded function.

Assumption 2 The time-varying scaling functions matrix $M(t) = (m_{ij}(t)) \in R^{m \times n}$ is a bounded matrix, and $m_{ij}(t)$ is a continuous bounded function or a constant.

3 Synchronization criteria

In this section, we will study the GFMPLS between two uncertain complex dynamical networks with dif-

ferent dimension of network nodes via adaptive control method.

From Eq. (3), the time derivative of $e_i(t)$ will be

$$\dot{e}_i(t) = \dot{y}_i(t) - \dot{M}(t)x_i(t - \tau(t))$$
$$- M(t)\dot{x}_i(t - \tau(t))(1 - \dot{\tau}(t)),$$
$$i = 1, 2, \ldots, N. \tag{6}$$

By substituting Eqs. (1) and (2) into Eq. (6), the error dynamical system is obtained as follows:

$$\dot{e}_i(t) = G_i(y_i(t))\Psi_i + g_i(y_i(t))$$
$$+ \sum_{j=1}^{N} d_{ij} Q(e_j(t) + M(t)x_j(t - \tau(t)))$$
$$+ u_i(t) - \dot{M}(t)x_i(t - \tau(t))$$
$$+ M(t)\dot{x}_i(t - \tau(t))\dot{\tau}(t)$$
$$- M(t)\left[F_i(x_i(t - \tau(t)))\Phi_i \right.$$
$$\left. + f_i(x_i(t - \tau(t))) + \sum_{j=1}^{N} c_{ij} P x_j(t - \tau(t)) \right] \tag{7}$$

where $i = 1, 2, \ldots, N$.

Theorem 1 *Given the time-varying scaling matrix $M(t) = (m_{ij}(t)) \in R^{m \times n}$, and the element in each row cannot be equal to zero at the same time, the GFMPLS between two uncertain complex dynamical networks (1) and (2) with different dimension of network nodes can be achieved by using the following adaptive controller:*

$$u_i(t) = \eta_i(t) - g_i(y_i(t)) + M(t)f_i(x_i(t - \tau(t)))$$
$$+ \dot{M}(t)x_i(t - \tau(t)) - M(t)\dot{x}_i(t - \tau(t))\dot{\tau}(t)$$
$$+ \sum_{j=1}^{N} (c_{ij}M(t)P - d_{ij}QM(t))x_j(t - \tau(t)),$$
$$i = 1, 2, \ldots, N, \tag{8}$$

where $\eta_i(t) = -G_i(y_i(t))\hat{\Psi}_i(t) + M(t)F_i(x_i(t - \tau(t)))\hat{\Phi}_i(t) - \beta_i(t)e_i(t)$.

The adaptive laws are

$$\dot{\hat{\Psi}}_i(t) = k_1 G_i^T(y_i(t))e_i(t), \tag{9}$$

$$\dot{\hat{\Phi}}_i(t) = -k_2 F_i^T(x_i(t - \tau(t)))M^T(t)e_i(t), \tag{10}$$

$$\dot{\beta}_i(t) = \lambda e_i^T(t)e_i(t), \quad for\ i = 1, 2, \ldots, N, \tag{11}$$

where k_1, k_2 and λ are positive control parameters, they can control the speed of convergence of synchronization errors. $\hat{\Psi}(t)$ and $\hat{\Phi}(t)$ are the estimated parameters for the nonlinear dynamical networks (1) *and* (2), *respectively. By putting the adaptive controller* (8) *and adaptive laws* (9)–(11) *into* (7), *the synchronization error dynamical system can be expressed by*

$$
\begin{aligned}
\dot{e}_i(t) = {} & G_i\big(y_i(t)\big)\big(\Psi_i - \hat{\Psi}_i(t)\big) \\
& - M(t)F_i\big(x_i\big(t - \tau(t)\big)\big)\big(\Phi_i - \hat{\Phi}_i(t)\big) \\
& + \sum_{j=1}^{N} d_{ij} Q e_j(t) - \beta_i(t) e_i(t)
\end{aligned}
\tag{12}
$$

where $i = 1, 2, \ldots, N$.

Proof Let $e(t) = (e_1(t), e_2(t), \ldots, e_N(t))^T \in R^{mN}$, and based on the adaptive controller (8), the update laws (9)–(11) and the synchronization error dynamical system (12), we construct the Lyapunov candidate function as follows:

$$
\begin{aligned}
V(t) = {} & \frac{1}{2} e^T(t) e(t) + \frac{1}{2} \sum_{i=1}^{N} \bigg[\frac{1}{k_1} \tilde{\Psi}_i^T(t) \tilde{\Psi}_i(t) \\
& + \frac{1}{k_2} \tilde{\Phi}_i^T(t) \tilde{\Phi}_i(t) + \frac{1}{\lambda} \tilde{\beta}_i^2(t) \bigg].
\end{aligned}
\tag{13}
$$

Denote $\tilde{\Psi}_i(t) = \hat{\Psi}_i(t) - \Psi_i$, $\tilde{\Phi}_i(t) = \hat{\Phi}_i(t) - \Phi_i$ and $\tilde{\beta}_i(t) = \beta_i(t) - \beta_i^*$ (where β_i^* is a positive constant that should be determined).

Obviously, $V(t) \geq 0$. Taking the time derivative of $V(t)$ along the trajectories of the synchronization error dynamical system (12), and using (8)–(11), we have

$$
\begin{aligned}
\dot{V}(t) = {} & \sum_{i=1}^{N} \bigg[e_i^T(t) \dot{e}_i(t) + \frac{1}{k_1} \dot{\tilde{\Psi}}_i^T(t) \tilde{\Psi}_i(t) \\
& + \frac{1}{k_2} \dot{\tilde{\Phi}}_i^T(t) \tilde{\Phi}_i(t) + \frac{1}{\lambda} \tilde{\beta}_i(t) \dot{\tilde{\beta}}_i(t) \bigg] \\
= {} & \sum_{i=1}^{N} \bigg[e_i^T(t) \bigg\{ G_i\big(y_i(t)\big)\big(\Psi_i - \hat{\Psi}_i(t)\big) \\
& - M(t) F_i\big(x_i\big(t - \tau(t)\big)\big)\big(\Phi_i - \hat{\Phi}_i(t)\big) \\
& + \sum_{j=1}^{N} d_{ij} Q e_j(t) - \beta_i(t) e_i(t) \bigg\}
\end{aligned}
$$

$$
\begin{aligned}
& + \frac{1}{k_1} \dot{\tilde{\Psi}}_i^T(t) \tilde{\Psi}_i(t) + \frac{1}{k_2} \dot{\tilde{\Phi}}_i^T(t) \tilde{\Phi}_i(t) \\
& + \frac{1}{\lambda} \tilde{\beta}_i(t) \dot{\beta}_i(t) \bigg] \\
= {} & \sum_{i=1}^{N} e_i^T(t) \big[-G_i\big(y_i(t)\big) \tilde{\Psi}_i(t) \\
& + M(t) F_i\big(x_i\big(t - \tau(t)\big)\big) \tilde{\Phi}_i(t) \big] \\
& + \sum_{i=1}^{N} \sum_{j=1}^{N} d_{ij} e_i^T(t) Q e_j(t) \\
& - \sum_{i=1}^{N} \beta_i(t) e_i^T(t) e_i(t) \\
& + \sum_{i=1}^{N} \bigg[\frac{1}{k_1} \big(k_1 e_i^T(t) G_i\big(y_i(t)\big) \tilde{\Psi}_i(t) \big) \\
& + \frac{1}{k_2} \big(-k_2 M(t) F_i\big(x_i\big(t - \tau(t)\big)\big) \big) \tilde{\Phi}_i(t) \\
& + \frac{1}{\lambda} \big(\beta_i(t) - \beta_i^* \big) \lambda e_i^T(t) e_i(t) \bigg] \\
= {} & \sum_{i=1}^{N} \sum_{j=1}^{N} d_{ij} e_i^T(t) Q e_j(t) - \sum_{i=1}^{N} \beta_i^* e_i^T(t) e_i(t) \\
\leq {} & \bigg(\lambda_{\max}\bigg(\frac{\hat{D} + \hat{D}^T}{2} \bigg) - \beta_{\min}^* \bigg) e^T(t) e(t) \\
= {} & (-\beta^{**}) e^T(t) e(t),
\end{aligned}
\tag{14}
$$

where $\hat{D} = D \otimes Q \in R^{mN \times mN}$, $\beta^{**} = \beta_{\min}^* - \lambda_{\max}(\frac{\hat{D}+\hat{D}^T}{2})$ and $\beta_{\min}^* = \min(\beta_i^*)$ $(i = 1, 2, \ldots, N)$.

It is obvious that there exist sufficiently large positive constants β_i^* $(i = 1, 2, \ldots, N)$ such that $\lambda_{\max}(\frac{\hat{D}+\hat{D}^T}{2}) < \beta_{\min}^*$, and then we can obtain $\beta^{**} > 0$. Namely, $\dot{V}(t) < 0$, i.e. $\lim_{t \to \infty} e(t) = 0$. Therefore, the GFMPLS between two uncertain dynamical networks (1) and (2) with different dimensions can be achieved by adaptive controller (8) and the adaptive laws (9)–(11). This completes the proof. $\square$

Based on Theorem 1, the following corollaries can be easily derived.

Corollary 1 *Assume that the time delay $\tau(t) = \tau > 0$ is constant, i.e., $\dot{\tau}(t) = 0$. For given the time-varying*

scaling matrix $M(t) = (m_{ij}(t)) \in R^{m \times n}$, and the element in each row cannot be equal to zero at the same time, the GFMPLS between two uncertain complex dynamical networks (1) and (2) with different dimension of network nodes can be achieved by using the following adaptive controller:

$$
\begin{aligned}
u_i(t) = {} & \eta_i(t) - g_i\big(y_i(t)\big) + M(t) f_i\big(x_i(t-\tau)\big) \\
& + \dot{M}(t) x_i(t-\tau) \\
& + \sum_{j=1}^{N} \big(c_{ij} M(t) P - d_{ij} Q M(t)\big) x_j(t-\tau),
\end{aligned}
\tag{15}
$$

where $\eta_i(t) = -G_i(y_i(t))\hat{\Psi}_i(t) + M(t) F_i(x_i(t-\tau)) \times \hat{\Phi}_i(t) - \beta_i(t) e_i(t)$.

The adaptive laws are (9)–(11).

Corollary 2 *Based on Corollary 1, assume that the time-varying scaling matrix $M(t) = (m_{ij}) \in R^{m \times n}$ is a constant matrix, i.e., $\dot{M}(t) = 0$, and the element in each row cannot be equal to zero at the same time, the GFMPLS between two uncertain complex dynamical networks (1) and (2) with different dimension of network nodes can be achieved by using the following adaptive controller:*

$$
\begin{aligned}
u_i(t) = {} & \eta_i(t) - g_i\big(y_i(t)\big) + M f_i\big(x_i(t-\tau)\big) \\
& + \sum_{j=1}^{N} (c_{ij} M P - d_{ij} Q M) x_j(t-\tau),
\end{aligned}
\tag{16}
$$

where $\eta_i(t) = -G_i(y_i(t))\hat{\Psi}_i(t) + M F_i(x_i(t-\tau)) \times \hat{\Phi}_i(t) - \beta_i(t) e_i(t)$.

The adaptive laws are (9)–(11).

Remark 2 In our work, the coupling configuration matrices C and D need not be symmetric or irreducible. In addition, there is not any constraint imposed on the inner coupling matrices P and Q. Furthermore, each node of the networks may have different local dynamics. The proposed approach is applicable to all kinds of complex dynamical networks.

Remark 3 The constant k_1, k_2 and λ can be chosen appropriately beforehand to adjust the synchronization rate. However, the inequality $\lambda_{\max}(\frac{\hat{D}+\hat{D}^T}{2}) < \beta_{\min}^*$ is just only a sufficient condition but not a necessary one.

4 Illustrative examples

In this section, some representative examples are performed to verify the effectiveness of the proposed synchronization scheme in the previous section. The total synchronization error is defined as

$$
E(t) = \sqrt{\sum_{i=1}^{N} \sum_{j=1}^{m} e_{ij}^2(t)}.
$$

The total synchronization error $E(t)$ is used to measure the quality of the synchronization process. It is obvious that when $\lim_{t \to \infty} E(t) = 0$, the drive and response networks achieve the desired synchronization globally.

In the simulations, the node equation of the drive network (1) is described by the following 10 three-dimensional chaotic systems [33]:

$$
\begin{aligned}
& \begin{bmatrix} \dot{x}_{i1}(t) \\ \dot{x}_{i2}(t) \\ \dot{x}_{i3}(t) \end{bmatrix} \\
& = \begin{bmatrix} x_{i2}(t) - x_{i1}(t) & 0 & 0 \\ 0 & 0 & x_{i2}(t) \\ 0 & -x_{i3}(t) & 0 \end{bmatrix} \begin{bmatrix} \varphi_{i1} \\ \varphi_{i2} \\ \varphi_{i3} \end{bmatrix} \\
& + \begin{bmatrix} -x_{i2}(t) x_{i3}(t) \\ (x_{i1}(t) - x_{i3}(t))^4 - 10 x_{i1}(t) x_{i3}(t) \\ x_{i1}^2(t) + x_{i2}^2(t) \end{bmatrix}, \\
& i = 1, 2, \ldots, 10,
\end{aligned}
\tag{17}
$$

where the real value of the unknown parameter vector is $\Phi_i = [\varphi_{i1} \ \varphi_{i2} \ \varphi_{i3}]^T = [35 \ 8 \ 28]^T$. When the parameter vector is set by default as $\Phi_i = [35 \ 8 \ 28]^T$, three Lyapunov Exponents (LEs) of the system (17) are $LE_1 = 2.8255, LE_2 = 0$ and $LE_3 = -17.831$. The system (17) behaves chaotically with one positive LE.

For the response network (2), 10 nodes are described by the following four-dimensional hyperchaotic Chen systems [34]:

$$
\begin{aligned}
& \begin{bmatrix} \dot{y}_{i1}(t) \\ \dot{y}_{i2}(t) \\ \dot{y}_{i3}(t) \\ \dot{y}_{i4}(t) \end{bmatrix} \\
& = \begin{bmatrix} y_{i2}(t) - y_{i1}(t) & 0 & 0 & 0 \\ 0 & 0 & y_{i2}(t) & 0 \\ 0 & -y_{i3}(t) & 0 & 0 \\ 0 & 0 & 0 & -y_{i1}(t) \end{bmatrix}
\end{aligned}
$$

$$\times \begin{bmatrix} \psi_{i1} \\ \psi_{i2} \\ \psi_{i3} \\ \psi_{i4} \end{bmatrix}$$

$$+ \begin{bmatrix} 0 \\ 4y_{i1}(t) - 10y_{i1}(t)y_{i3}(t) + 4y_{i4}(t) \\ y_{i2}^2(t) \\ 0 \end{bmatrix},$$

$$i = 1, 2, \ldots, 10, \tag{18}$$

where the real value unknown parameter vector is $\Psi_i = [\psi_{i1}\ \psi_{i2}\ \psi_{i3}\ \psi_{i4}]^T = [35\ 3\ 21\ 2]^T$. When the parameter vector is set by default as $\Psi_i = [35\ 3\ 21\ 2]^T$, four LEs of the system (18) are $LE_1 = 1.360$, $LE_2 = 0.258$, $LE_3 = 0$ and $LE_4 = -20.851$. The system (18) behaves as hyperchaos with two positive LEs.

4.1 GFMPLS between a full coupled network and a tree coupled network

A full coupled network and a tree coupled network are drawn in Figs. 1 and 2. They are used as the drive and response networks, respectively. The coupling configuration matrices are given, respectively, as follows:

$$C = \begin{bmatrix} -9 & 1 & 1 & 1 & 1 & 1 & 1 & 1 & 1 & 1 \\ 1 & -9 & 1 & 1 & 1 & 1 & 1 & 1 & 1 & 1 \\ 1 & 1 & -9 & 1 & 1 & 1 & 1 & 1 & 1 & 1 \\ 1 & 1 & 1 & -9 & 1 & 1 & 1 & 1 & 1 & 1 \\ 1 & 1 & 1 & 1 & -9 & 1 & 1 & 1 & 1 & 1 \\ 1 & 1 & 1 & 1 & 1 & -9 & 1 & 1 & 1 & 1 \\ 1 & 1 & 1 & 1 & 1 & 1 & -9 & 1 & 1 & 1 \\ 1 & 1 & 1 & 1 & 1 & 1 & 1 & -9 & 1 & 1 \\ 1 & 1 & 1 & 1 & 1 & 1 & 1 & 1 & -9 & 1 \\ 1 & 1 & 1 & 1 & 1 & 1 & 1 & 1 & 1 & -9 \end{bmatrix},$$

$$D = \begin{bmatrix} -9 & 1 & 1 & 1 & 1 & 1 & 1 & 1 & 1 & 1 \\ 1 & 0 & 0 & 0 & 0 & & & & & \\ 1 & -3 & 0 & 0 & 1 & 1 & 0 & 0 & 0 & 0 \\ 1 & 0 & -3 & 0 & 0 & 0 & 1 & 1 & 0 & 0 \\ 1 & 0 & 0 & -3 & 0 & 0 & 0 & 0 & 1 & 1 \\ 0 & 1 & 0 & 0 & -1 & 0 & 0 & 0 & 0 & 0 \\ 0 & 1 & 0 & 0 & 0 & -1 & 0 & 0 & 0 & 0 \\ 0 & 0 & 1 & 0 & 0 & 0 & -1 & 0 & 0 & 0 \\ 0 & 0 & 1 & 0 & 0 & 0 & 0 & -1 & 0 & 0 \\ 0 & 0 & 0 & 1 & 0 & 0 & 0 & 0 & -1 & 0 \\ 0 & 0 & 0 & 1 & 0 & 0 & 0 & 0 & 0 & -1 \end{bmatrix}.$$
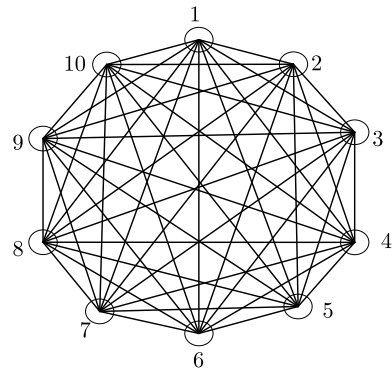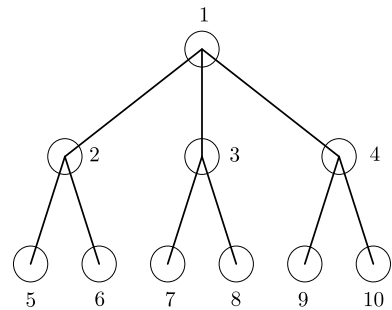

Fig. 1 A full coupled network

Fig. 2 A tree coupled network

The inner coupling matrices are taken arbitrarily as $P = \mathrm{diag}(2, 4, 6)$ and $Q = \mathrm{diag}(0.2, 1, -0.8, -5)$. It is easy to obtain $\lambda_{\max}(\frac{\hat{D}+\hat{D}^T}{2}) = 25$.

We choose the time delay $\tau(t) = 0.1 - 0.02e^{-t} \times \sqrt{2e^t}$, the control parameters $k_1 = 25$, $k_2 = 25$ and $\lambda = 15$, and the time-varying scaling function matrix

$$M(t) = \begin{bmatrix} 1+\sin(5t) & 2 & -3\cos(2t) \\ -1 & 0.8+\sin(3t) & 0.5 \\ 3\cos(4t) & -0.5\cos(3t) & 2\sin(t) \\ 1 & -2 & 3\sin(3t) \end{bmatrix}.$$

By using the adaptive controller (8) and update laws (9)–(11), GFMPLS between a full coupled network and a tree coupled network can be realized as displayed in Figs. 3, 4, 5. Figure 3 displays the time evolution curves of the synchronization errors $e_i(t)$ and $E(t)$, which indicates that GFMPLS between a full coupled network and a tree coupled network is achieved. Moreover, we can observe that

Fig. 3 Time evolution
curves of the
synchronization errors
between a full coupled
network and a tree coupled
network (**a**) e_{i1}, (**b**) e_{i2},
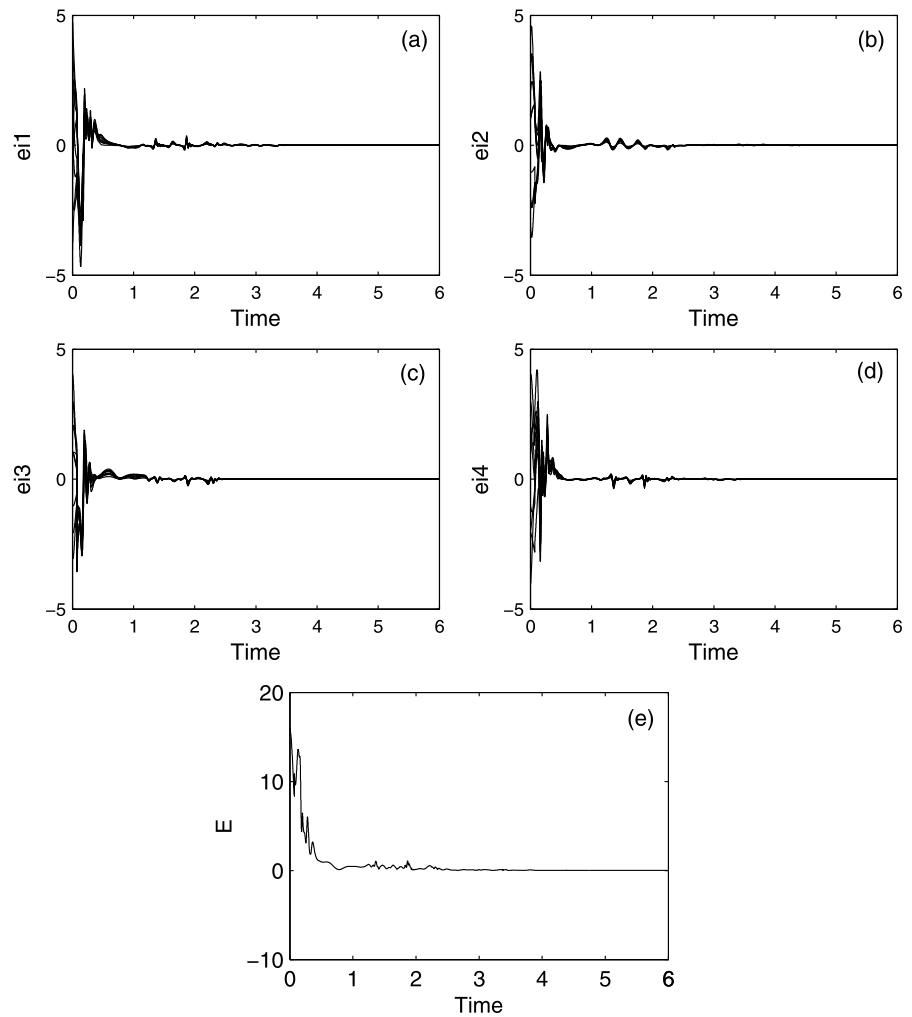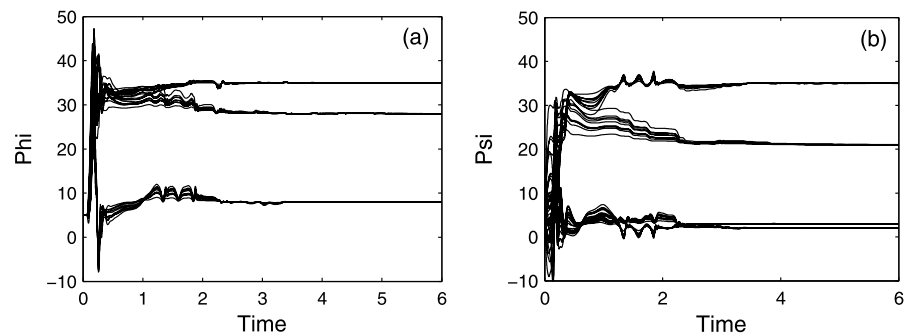(**c**) e_{i3}, (**d**) e_{i4}, (**e**) $E(t)$

Fig. 4 Time evolution
curves of the estimated
parameters: (**a**) $\hat{\Phi}_i(t)$,
(**b**) $\hat{\Psi}_i(t)$

the estimated parameters ($\hat{\Phi}_i(t)$ and $\hat{\Psi}_i(t)$) of drive
and response networks converge to their real values
$\Phi_i = [35\ 8\ 28]^T$ and $\Psi_i = [35\ 3\ 21\ 2]^T$ in Fig. 4.

From Fig. 5, we can see that the controlling strengths
$\beta_i(t)$ are adjusted to fixed values in a very short
time.
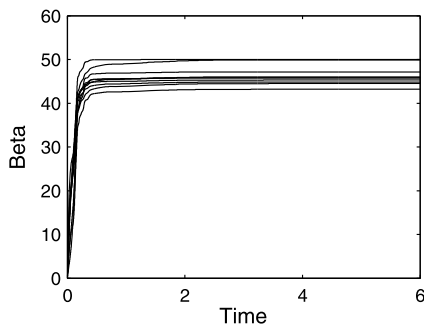
Fig. 5 Time evolution curves of the controlling strengths $\beta_i(t)$
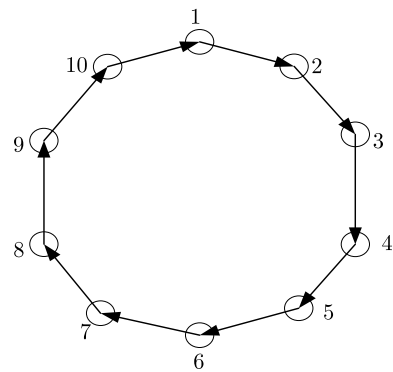
Fig. 6 A directed ring coupled network

4.2 GFMPLS between a directed ring coupled network and a star coupled network

A directed ring coupled network and a star coupled network are drawn in Figs. 6 and 7. They are used as the drive and response networks, respectively. The coupling configuration matrices are given, respectively, as follows:

$$
C = \begin{bmatrix}
-9 & 1 & 1 & 1 & 1 & 1 & 1 & 1 & 1 & 1 \\
1 & -1 & 0 & 0 & 0 & 0 & 0 & 0 & 0 & 0 \\
0 & 1 & -1 & 0 & 0 & 0 & 0 & 0 & 0 & 0 \\
0 & 0 & 1 & -1 & 0 & 0 & 0 & 0 & 0 & 0 \\
0 & 0 & 0 & 1 & -1 & 0 & 0 & 0 & 0 & 0 \\
0 & 0 & 0 & 0 & 1 & -1 & 0 & 0 & 0 & 0 \\
0 & 0 & 0 & 0 & 0 & 1 & -1 & 0 & 0 & 0 \\
0 & 0 & 0 & 0 & 0 & 0 & 1 & -1 & 0 & 0 \\
0 & 0 & 0 & 0 & 0 & 0 & 0 & 1 & -1 & 0 \\
0 & 0 & 0 & 0 & 0 & 0 & 0 & 0 & 1 & -1
\end{bmatrix},
$$

$$
D = \begin{bmatrix}
-9 & 1 & 1 & 1 & 1 & 1 & 1 & 1 & 1 & 1 \\
1 & 1 & 1 & 1 & 1 & & & & & \\
1 & -1 & 0 & 0 & 0 & 0 & 0 & 0 & 0 & 0 \\
1 & 0 & -1 & 0 & 0 & 0 & 0 & 0 & 0 & 0 \\
1 & 0 & 0 & -1 & 0 & 0 & 0 & 0 & 0 & 0 \\
1 & 0 & 0 & 0 & -1 & 0 & 0 & 0 & 0 & 0 \\
1 & 0 & 0 & 0 & 0 & -1 & 0 & 0 & 0 & 0 \\
1 & 0 & 0 & 0 & 0 & 0 & -1 & 0 & 0 & 0 \\
1 & 0 & 0 & 0 & 0 & 0 & 0 & -1 & 0 & 0 \\
1 & 0 & 0 & 0 & 0 & 0 & 0 & 0 & -1 & 0 \\
1 & 0 & 0 & 0 & 0 & 0 & 0 & 0 & 0 & -1
\end{bmatrix}.
$$

The inner coupling matrices are taken arbitrarily as $P = \mathrm{diag}(-1, 2, 3)$ and $Q = \mathrm{diag}(1, -2, 0.2, 4)$. It is easy to obtain $\lambda_{\max}(\frac{\hat{D}+\hat{D}^T}{2}) = 20$.
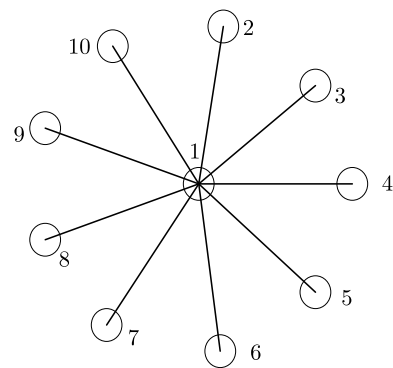

Fig. 7 A star coupled network

We choose the time delay $\tau(t) = 0.6 - \frac{e^{2t}}{2+2e^{2t}}$, the control parameters $k_1 = 30$, $k_2 = 30$ and $\lambda = 10$, and the time-varying scaling function matrix

$$
M(t) = \begin{bmatrix}
\cos(2t) & 3\cos(6t) & -3 \\
3 & 1.5 + \sin(2t) & -1.8 \\
2\sin(3t) & 3 - 2.5\cos(4t) & 2\sin(t) \\
\cos(4t) & -4 & -3\sin(t)
\end{bmatrix}.
$$

By using the adaptive controller (8) and update laws (9)–(11), GFMPLS between a directed ring coupled network and a star coupled network can be realized as displayed in Figs. 8, 9, 10. Figure 8 displays the time evolution curves of the synchronization errors $e_i(t)$ and $E(t)$, which indicates that GFMPLS between a directed ring coupled network and a star coupled network is achieved. Moreover, we can observe that the estimated parameters ($\hat{\Phi}_i(t)$ and $\hat{\Psi}_i(t)$) of drive

Fig. 8 Time evolution
curves of the
synchronization errors
between a directed ring
coupled network and a star
coupled network (**a**) e_{i1},
(**b**) e_{i2}, (**c**) e_{i3}, (**d**) e_{i4},
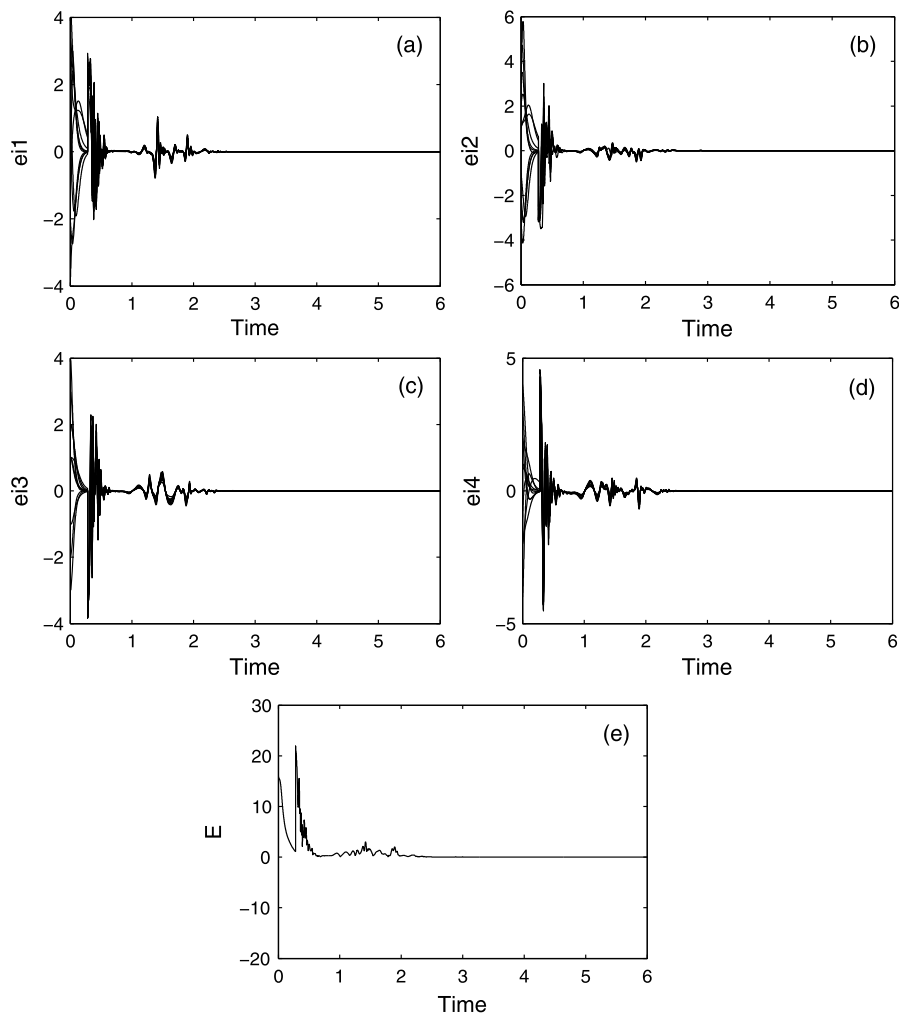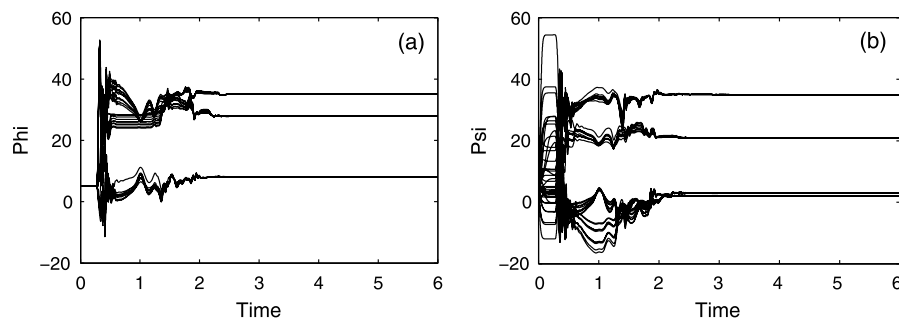(**e**) $E(t)$

Fig. 9 Time evolution
curves of the estimated
parameters: (**a**) $\hat{\Phi}_i(t)$,
(**b**) $\hat{\Psi}_i(t)$

network and response network converge to theirin
real values $\Phi_i = [35\ 8\ 28]^T$ and $\Psi_i = [35\ 3\ 21\ 2]^T$
Fig. 9. From Fig. 10, we can see that the controlling
strengths $\beta_i(t)$ are adjusted to fixed values in a very
short time.

4.3 GFMPLS between two directed complex networks

Two different directed complex networks are drawn
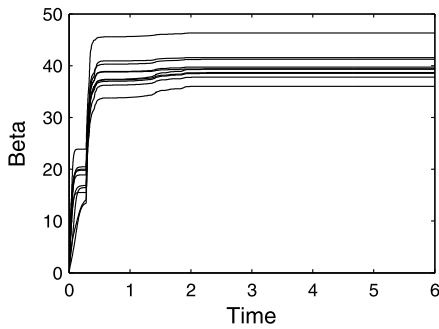in Figs. 11 and 12. They are used as the drive and

Fig. 10 Time evolution curves of the controlling strengths $\beta_i(t)$

response networks, respectively. The coupling configuration matrices are given, respectively, as follows:

$$C = \begin{bmatrix} -2 & 0 & 0 & 0 & 0 & 1 & 0 & 0 & 1 & 0 \\ 0 & -4 & 1 & 0 & 0 & 0 & 0 & 1 & 1 & 1 \\ 0 & 0 & -3 & 0 & 1 & 0 & 1 & 1 & 0 & 0 \\ 1 & 1 & 1 & -4 & 0 & 0 & 0 & 1 & 0 & 0 \\ 0 & 0 & 1 & 0 & -2 & 1 & 0 & 0 & 0 & 0 \\ 0 & 1 & 0 & 1 & 0 & -2 & 0 & 0 & 0 & 0 \\ 0 & 0 & 0 & 0 & 1 & 0 & -1 & 0 & 0 & 0 \\ 1 & 0 & 0 & 0 & 0 & 1 & 0 & -2 & 0 & 0 \\ 1 & 0 & 0 & 1 & 0 & 1 & 1 & 0 & -4 & 0 \\ 0 & 0 & 0 & 0 & 1 & 0 & 0 & 1 & 0 & -2 \end{bmatrix},$$

$$D = \begin{bmatrix} -2 & 0 & 0 & 0 & 0 & 1 & 0 & 0 & 0 & 1 \\ 1 & -3 & 0 & 0 & 0 & 1 & 0 & 1 & 0 & 0 \\ 0 & 1 & -3 & 0 & 0 & 0 & 1 & 0 & 1 & 0 \\ 1 & 1 & 1 & -4 & 0 & 0 & 1 & 0 & 0 & 0 \\ 0 & 0 & 1 & 1 & -3 & 0 & 0 & 0 & 0 & 1 \\ 0 & 0 & 0 & 0 & 1 & -3 & 0 & 1 & 0 & 1 \\ 0 & 0 & 0 & 0 & 0 & 1 & -1 & 0 & 0 & 0 \\ 1 & 0 & 0 & 1 & 0 & 0 & 1 & -3 & 0 & 0 \\ 1 & 0 & 0 & 1 & 0 & 1 & 0 & 1 & -4 & 0 \\ 0 & 0 & 0 & 0 & 0 & 0 & 0 & 0 & 1 & -1 \end{bmatrix}.$$

The inner coupling matrices are taken arbitrarily as $P = \operatorname{diag}(0.1, 0.2, 0.3)$ and $Q = \operatorname{diag}(-3, 2, 0.5, 0.8)$. It is easy to obtain $\lambda_{\max}(\frac{\hat{D}+\hat{D}^T}{2}) = 14.8964$.

We choose the time delay $\tau(t) = 0.2e^{-t}\sqrt{3e^t} - \frac{e^t}{2+2e^t}$, the control parameters $k_1 = k_2 = \lambda = 30$, and the time-varying scaling function matrix

$$M(t) = \begin{bmatrix} \sin(t) & 2\sin(2t) & 1 - 0.3\cos(5t) \\ 1 & \sin(3t) & 2.5 \\ 2\cos(4t) & 2 - 0.5\sin(3t) & \sin(t) \\ \cos(2t) & 2 & -3\sin(2t) \end{bmatrix}.$$
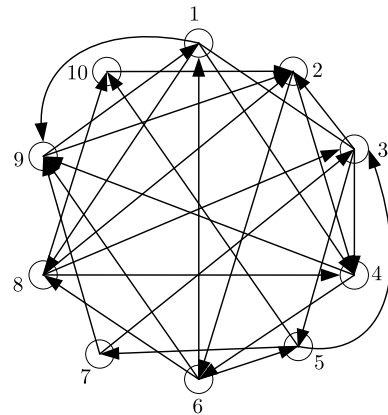

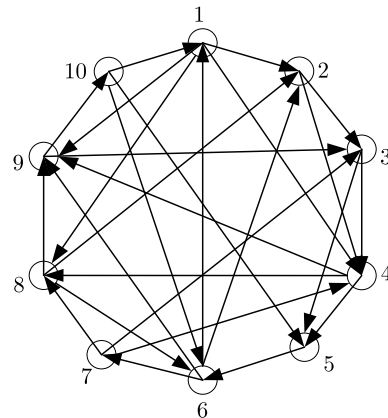**Fig. 11** The drive network

Fig. 12 The response network

By using the adaptive controller (8) and update laws (9)–(11), GFMPLS between two directed complex networks can be realized as displayed in Figs. 13, 14, 15. Figure 13 displays the time evolution curves of the synchronization errors $e_i(t)$ and $E(t)$, which indicates that GFMPLS between two different directed complex networks is achieved. Moreover, we can observe that the estimated parameters ($\hat{\Phi}_i(t)$ and $\hat{\Psi}_i(t)$) of drive network and response network converge to their real values $\Phi_i = [35\ 8\ 28]^T$ and $\Psi_i = [35\ 3\ 21\ 2]^T$ i n Fig. 14. From Fig. 15, we can see that the controlling strengths $\beta_i(t)$ are adjusted to fixed values in a very short time.

Fig. 13 Time evolution
curves of the
synchronization errors
between two different
directed complex networks
(**a**) e_{i1}, (**b**) e_{i2}, (**c**) e_{i3},
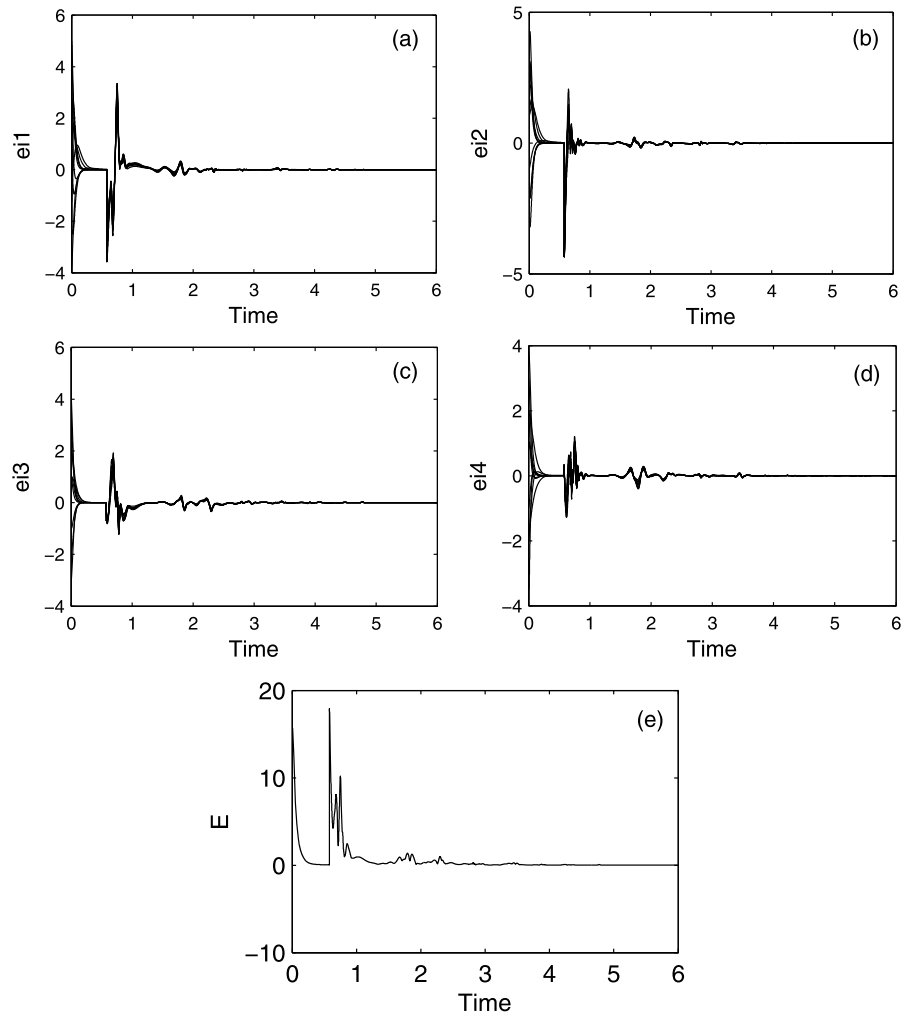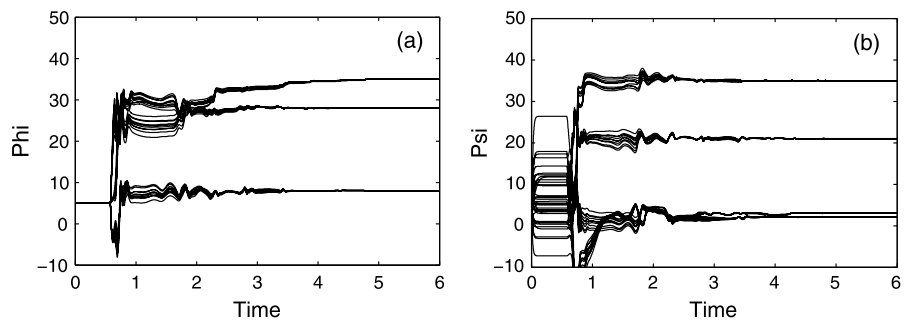(**d**) e_{i4}, (**e**) $E(t)$

Fig. 14 Time evolution
curves of the estimated
parameters: (**a**) $\hat{\Phi}_i(t)$,
(**b**) $\hat{\Psi}_i(t)$

4.4 GFMPLS between two directed complex networks with time-varying coupling matrices

4.4.1 Network topology structure is unchanged

In this section, we further test the performance of the proposed method in the case that the topology structure of the complex network is unchanged but the value of coupling strength is time-varying. For the coupling configuration matrices C and D, and the inner coupling matrices P and Q, they may also be a time-varying function matrices. The proposed approach is still applicable to this situation.

The inner coupling matrices are taken arbitrarily as follows:

$$P = \begin{bmatrix} 0.3 - 0.1\sin(t) & 0 & 0 \\ 0 & 0.2 - 0.1\sin(2t) & 0 \\ 0 & 0 & 0.1 + 0.02\cos(5t) \end{bmatrix},$$

$$Q = \begin{bmatrix} 0.2 + 0.1\sin(2t) & 0 & 0 & 0 \\ 0 & 0.2 + 0.1\sin(3t) & 0 & 0 \\ 0 & 0 & 0.2 - 0.1\cos(4t) & 0 \\ 0 & 0 & 0 & 0.3 - 0.2\sin(2t)] \end{bmatrix}.$$

The coupling configuration matrices are given, respectively, as follows:

$$C = \begin{bmatrix} -2 - 0.2\sin(t) & 0 & 0 & 0 & 1 + 0.1\sin(t) & 0 \\ 0 & -3 & 0 & 0 & 0 & 1 \\ 1 & 1 + 0.1\sin(t) & -2 - 0.1\sin(t) & 0 & -1 + 0.1\sin(t) & 0 \\ 0 & 1 & 0 & -2 & 0 & 0 \\ 0.5\sin(t) - 1 & 0 & 0 & 0 & 5 - 2\sin(t) & 0 \\ 0 & 0 & 0 & 1 & 0 & -1 \\ 0.2\sin(t) - 1 & 0 & 0 & 0 & 0.1\sin(t) - 2 & 0 \\ 0 & 1 & 0 & 1 & 0 & 1 \\ 0 & 2 + \sin(t) & 0 & 0 & 2 + \sin(t) & 1 \\ 0 & 1 & 0 & 2 & 0 & 1 \end{bmatrix}$$

$$\begin{bmatrix} 1 + 0.1\sin(t) & 0 & 0 & 0 \\ 0 & 1 & 1 & 0 \\ 0 & 1 - 0.1\sin(t) & 0 & 0 \\ 0 & 1 & 0 & 0 \\ 0 & 1.5\sin(t) - 4 & 0 & 0 \\ 0 & 0 & 0 & 0 \\ 5 - 0.5\sin(t) & 0 & 0.2\sin(t) - 2 & 0 \\ 0 & -4 & 1 & 0 \\ 0 & 0 & -5 - 2\sin(t) & 0 \\ 0 & 1 & 0 & -5 \end{bmatrix},$$

$$D = \begin{bmatrix} -5 - 3\sin(2t) & 0 & 0 & 2 + \sin(2t) & 0 & 0 \\ 0 & -4 - 2\cos(t) & 0 & 0 & 0 & 2 + \cos(t) \\ 1 & 1 + 0.2\sin(2t) & -5 & 0 & 0 & 2 \\ 0 & 0 & 0.5\sin(3t) - 1 & 3 - 2\sin(3t) & 0 & 0 \\ 0 & 2 & 0 & 1 - 0.1\cos(t) & -6 & 0 \\ 0 & \sin(t) - 2 & 0 & 0 & 0 & 2 - \sin(t) \\ 0 & 1 & 0 & 0 & 1 & 0 \\ 0 & 0 & \sin(2t) - 3 & 0 & 0 & 0 \\ 1 + 0.5\sin(5t) & 0 & 0 & 1 - 0.5\sin(5t) & 0 & 1 \\ 1 & 1 + 0.2\sin(t) & 1 & 0 & 0 & -0.2\sin(t) - 1 \end{bmatrix}$$

$$\begin{bmatrix} 3 + 2\sin(2t) & 0 & 0 & 0 \\ 0 & 2 + \cos(t) & 0 & 0 \\ 0 & 0 & 1 - 0.2\sin(2t) & 0 \\ 1.5\sin(3t) - 2 & 0 & 0 & 0 \\ 1 & 0 & 1 & 1 + 0.1\cos(t) \\ 0 & 0 & 0 & 0 \\ -4 & 0 & 1 & 1 \\ \sin(2t) - 2 & 5 - \sin(2t) & 0 & 0 \\ 1 & 0 & -4 & 0 \\ 0 & 2 & 1 & -5 \end{bmatrix}.$$

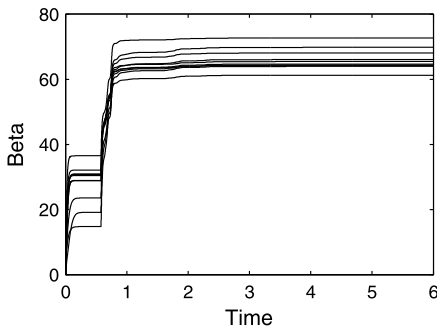It is easy to obtain $\lambda_{\max}(\frac{\hat{D} + \hat{D}^T}{2}) = 24.7154$.

Fig. 15 Time evolution curves of the controlling strengths $\beta_i(t)$

We choose the time delay $\tau(t) = 0.2e^{-t}\sqrt{3e^t} - \frac{e^t}{2 + 2e^t}$, the control parameters $k_1 = k_2 = \lambda = 30$, and the time-varying scaling function matrix

$$M(t) = \begin{bmatrix} \sin(t) & 2\sin(2t) & 1 - 0.3\cos(5t) \\ 1 & \sin(3t) & 2.5 \\ 2\cos(4t) & 2 - 0.5\sin(3t) & \sin(t) \\ \cos(2t) & 2 & -3\sin(2t) \end{bmatrix}.$$

By using the adaptive controller (8) and update laws (9)–(11), GFMPLS between two directed complex networks with time-varying coupling matrices can be realized as displayed in Figs. 16, 17, 18. Figure 16 displays the time evolution curves of the synchronization errors $e_i(t)$ and $E(t)$, which indicates that GFMPLS between two different directed complex networks with time-varying coupling matrices is achieved. Moreover, we can observe that the estimated parameters ($\hat{\Phi}_i(t)$ and $\hat{\Psi}_i(t)$) of drive network and response network converge to their real values $\Phi_i = [35\ 8\ 28]^T$ and $\Psi_i = [35\ 3\ 21\ 2]^T$ in Fig. 17. From Fig. 18, we can see that the controlling strengths $\beta_i(t)$ are adjusted to fixed values in a very short time.

4.4.2 Network structure with switching topology

Based on Sect. 4.4.1, suppose that at $t = 6$ the coupling configuration matrices C and D are switched to the following structures:

$$C' = \begin{bmatrix}
-4-0.2\sin(2t) & 0 & 0 & 2-0.2\sin(2t) & 0 \\
1-0.1\sin(t) & -2 & 0 & 1-0.2\sin(t) & 0 \\
0 & 1+0.1\sin(t) & -4-0.2\sin(t) & 0 & 1+0.1\sin(t) \\
-1 & 1 & 0 & -4 & 0 \\
0.1\cos(3t)-1 & 0 & 1-0.2\cos(3t) & 0 & 1-0.4\cos(3t) \\
0 & 1 & 0 & 1 & 0 \\
0 & 0 & 1-0.1\sin(2t) & 0 & 1+0.1\sin(2t) \\
1-0.2\cos(t) & 1 & -2 & 1 & 0 \\
0 & 2+0.5\sin(t) & 0 & 0 & -2 \\
0 & 1 & 0 & 0 & 0
\end{bmatrix}$$

$$\begin{bmatrix}
0 & 1+0.5\sin(2t) & 0 & 0 & 1-0.1\sin(2t) \\
-1 & 0 & 1+0.3\sin(t) & 0 & 0 \\
0 & 0 & 1 & 1 & 0 \\
1 & 0 & 1 & 0 & 2 \\
0 & 1 & 0.5\cos(3t)-2 & 0 & 0 \\
-2 & 0 & 0 & 1 & -1 \\
0 & -1 & 0 & 0 & -1 \\
0 & 0 & -3 & 1+0.2\cos(t) & 1 \\
1-0.2\sin(t) & 0 & 0 & -1-0.3\sin(t) & 0 \\
0 & 0 & 1 & 1 & -3
\end{bmatrix},$$

$$D' = \begin{bmatrix}
-4 & 0 & 2-\sin(2t) & 0 & 0 & 0 \\
0 & -3-0.5\cos(t) & -1 & 2+0.2\cos(t) & 0 & 0 \\
0 & 1+0.2\sin(3t) & -4 & 1 & 0 & 1-0.2\sin(3t) \\
1-0.5\sin(3t) & 2 & 0 & 0 & -1-0.3\sin(3t) & 0 \\
0 & 2 & 0 & 1-0.1\cos(t) & -6 & 0 \\
0 & \sin(t)-2 & 0 & 0 & 0 & 2-\sin(t) \\
1 & -1 & 0 & 0 & 1 & 0 \\
0 & 0 & 0 & 0 & \sin(2t)-3 & 0 \\
1+0.5\sin(5t) & 0 & 1 & 1-0.5\sin(5t) & 0 & 0 \\
0 & -0.2\sin(t)-1 & 0 & 1 & 1+0.2\sin(t) & 1
\end{bmatrix}$$

$$\begin{bmatrix}
1+0.5\sin(2t) & 0 & 1+0.5\sin(2t) & 0 \\
1 & 0 & 0 & 1+0.3\cos(t) \\
0 & 1 & 0 & 0 \\
0 & 0.8\sin(3t)-2 & 0 & 0 \\
1 & 0 & 1 & 1+0.1\cos(t) \\
0 & 0 & 0 & 0 \\
-5 & 1 & 2 & 1 \\
1 & 0 & -5 & 1 \\
\sin(2t)-2 & 5-2\sin(2t) & 0 & 0 \\
0 & 1 & 1 & -4
\end{bmatrix}.$$

Fig. 16 Time evolution curves of the synchronization errors between two different directed complex networks with time-varying coupling matrices (**a**) e_{i1}, (**b**) e_{i2}, (**c**) e_{i3}, (**d**) e_{i4}, (**e**) $E(t)$
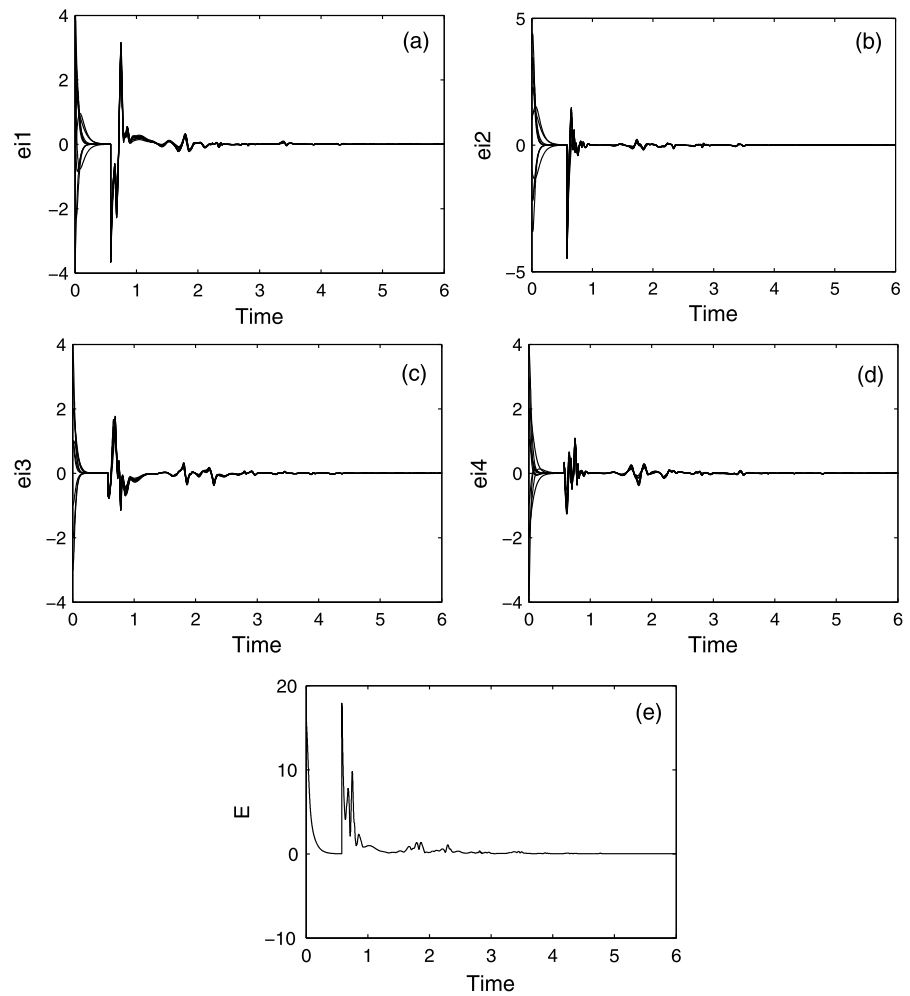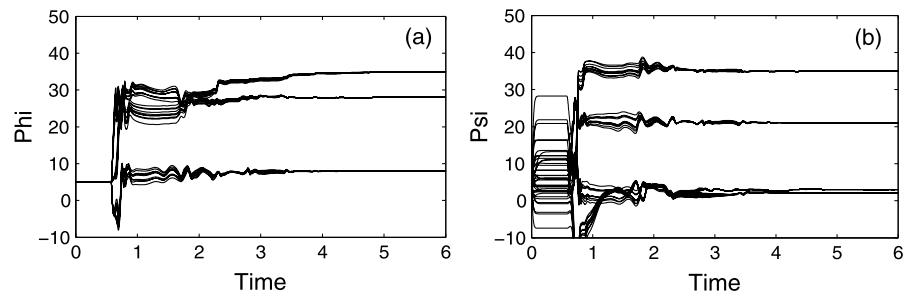
Fig. 17 Time evolution curves of the estimated parameters: (**a**) $\hat{\Phi}_i(t)$, (**b**) $\hat{\Psi}_i(t)$

By using the adaptive controllers (8) and update laws (9)–(11), GFMPLS between two directed complex networks with time-varying coupling matrices and switching topology can be realized as displayed in Figs. 19, 20, 21. Figure 19 displays the time evo-

lution curves of the synchronization errors $e_i(t)$ and $E(t)$, which indicates that GFMPLS between two different directed complex networks with time-varying coupling matrices and switching topology is achieved. Moreover, we can observe that the estimated parame-

ters ($\hat{\Phi}_i(t)$ and $\hat{\Psi}_i(t)$) of drive network and response network converge to their real values $\Phi_i = [35\ 8\ 28]^T$ and $\Psi_i = [35\ 3\ 21\ 2]^T$ in Fig. 20. From Fig. 21, we can see that the controlling strengths $\beta_i(t)$ are adjusted to fixed values in a very short time.

The above examples are simulated to verify the effectiveness of the proposed synchronization method in this paper. The first three examples are performed to illustrate the proposed synchronization method can adapt to the synchronization between undirected coupled network and undirected coupled network, directed coupled network and undirected coupled network, directed coupled network and directed coupled network, respectively. The last two examples are performed to illustrate the proposed synchronization method can adapt to the synchronization between two directed complex networks with time-varying coupling matrices and switching topology. From the above numerical simulation results, the limit of the synchronization error $e_i(t)$ asymptotically approaches zero.
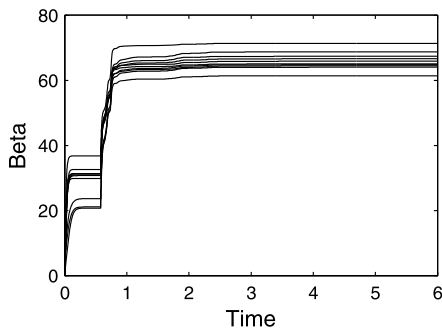

Fig. 18 Time evolution curves of the controlling strengths $\beta_i(t)$

Fig. 19 Time evolution curves of the synchronization errors between two different directed complex networks with time-varying coupling matrices and switching topology (**a**) e_{i1}, (**b**) e_{i2}, (**c**) e_{i3}, (**d**) e_{i4}, (**e**) $E(t)$
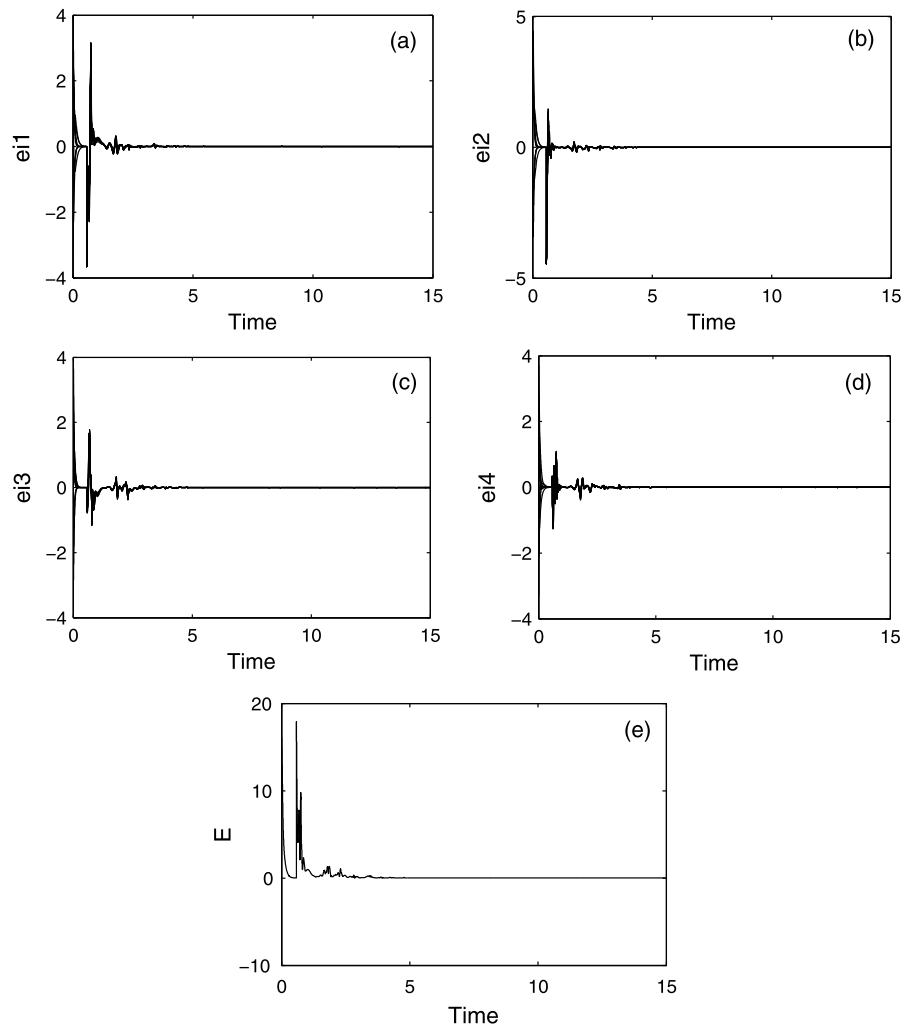
Fig. 20 Time evolution
curves of the estimated
parameters: (**a**) $\hat{\Phi}_i(t)$,
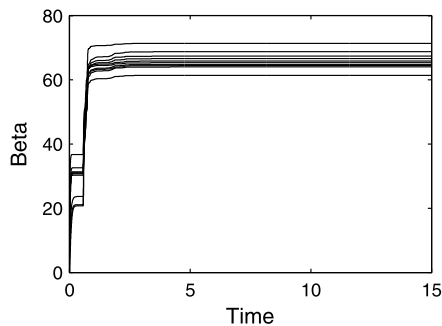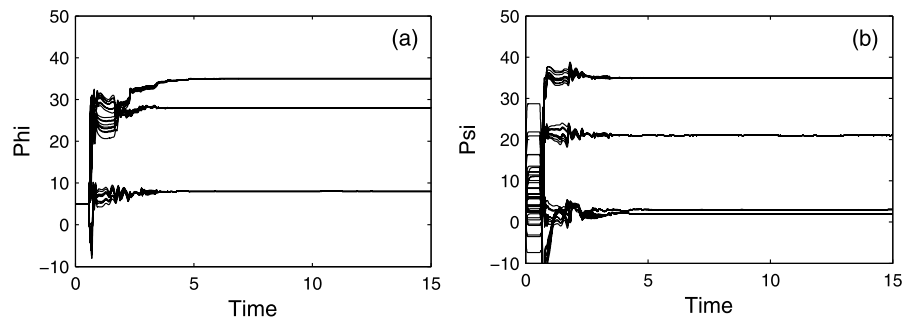(**b**) $\hat{\Psi}_i(t)$

Fig. 21 Time evolution curves of the controlling strengths $\beta_i(t)$

That is to say, generalized function matrix projective lag synchronization between two completely different complex dynamical networks with different dimension of network nodes can be accomplished by the proposed controller (8) and update laws (9)–(11), even if both the drive network and the response network have unknown parameters and time-varying coupling matrices or switching topology. In addition, the estimated parameters of the drive network $\hat{\Phi}_i(t)$ converge to their real values $\Phi_i = [35\ 8\ 28]^T$, and the estimated parameters of the response network $\hat{\Psi}_i(t)$ converge to their real values $\Psi_i = [35\ 3\ 21\ 2]^T$. The controlling strengths $\beta_i(t)$ are adjusted to fixed values in a very short time.

5 Conclusions

In this paper, we investigate generalized function matrix projective lag synchronization (GFMPLS) between two uncertain complex dynamical networks with different dimension of network nodes. The traditional model of the synchronization that a variable of response dynamical networks only corresponding to a variable of drive dynamical networks during the syn-

chronization process is broken by the matrix synchronization. GFMPLS includes projective synchronization (PS), lag synchronization (LS), function projective synchronization (FPS), matrix projective synchronization (MPS) and generalized function projective synchronization (GFPS), and it is a more general form of generalized synchronization. Based on Lyapunov stability theory, an adaptive controller is obtained and unknown parameters of both the drive network and the response network are estimated by update laws. Moreover, the three-dimension chaotic system and the four-dimension hyperchaotic system, respectively, as the nodes of the drive and response networks are analyzed in detail, and numerical simulation results are presented to illustrate the effectiveness of the theoretical results. In addition, the estimated parameters of uncertain complex dynamical networks can converge to their real values. The illustrative examples show that this method is effective in complex network with time-varying coupling matrices and static or switching topology.

In some practical engineering, networks often need to be controlled to a stable state. Chaos control and synchronization could be realized by using the same method in [35, 36]. In fact, network control and network synchronization are the same in essence. Consequently, complex network control and synchronization could also be realized by using the same method. In [37], the author designed the controller with one-dimensional, and the four-dimensional hyperchaotic system can be effectively controlled under this one-dimensional nonlinear controller. Therefore, considering the problem of application more convenient in the industrial field, we should further simplify the controller (reduce the dimension of the controller) in our future work. Moreover, the authors studied synchronization between integer-order chaotic system and fractional-order chaotic system in [38, 39]. This is a

great inspiration to us, and generalized function matrix projective lag synchronization between fractional-order and integer-order complex networks will be studied in our future work.

References

1. Watts, D.J., Strogatz, S.H.: Collective dynamics of small-world networks. Nature **393**, 440–442 (1998)
2. Barbaasi, A.L., Albert, R.: Emergence of scaling in random networks. Science **286**, 509–512 (1999)
3. Pecora, L., Carroll, T.: Synchronization in chaotic systems. Phys. Rev. Lett. **64**, 821–824 (1990)
4. Chen, D.Y., Zhang, R.F., Ma, X.Y., Liu, S.: Chaotic synchronization and anti-synchronization for a novel class of multiple chaotic systems via a sliding mode control scheme. Nonlinear Dyn. **69**, 35–55 (2012)
5. Ma, C., Wang, X.Y.: Impulsive control and synchronization of a new unified hyperchaotic system with varying control gains and impulsive intervals. Nonlinear Dyn. **70**, 551–558 (2012)
6. Yu, W.W., Cao, J.D.: Adaptive synchronization and lag synchronization of uncertain dynamical system with time delay based on parameter identification. Physica A **375**, 467–482 (2007)
7. Feng, C.F.: Projective synchronization between two different time-delayed chaotic systems using active control approach. Nonlinear Dyn. **62**, 453–459 (2010)
8. Gu, L., Zhang, X.D., Zhou, Q.: Consensus and synchronization problems on small-world networks. J. Math. Phys. **51**, 082701 (2010)
9. Fan, J., Wang, X.F.: On synchronization in scale-free dynamical networks. Physica A **349**, 443–451 (2005)
10. Sun, M., Zeng, C.Y., Tian, L.X.: Linear generalized synchronization between two complex networks. Commun. Nonlinear Sci. Numer. Simul. **15**, 2162–2167 (2010)
11. Zheng, S., Wang, S.G., Dong, G.G., Bi, Q.S.: Adaptive synchronization of two nonlinearly coupled complex dynamical networks with delayed coupling. Commun. Nonlinear Sci. Numer. Simul. **17**, 284–291 (2012)
12. Hu, C., Yu, J., Jiang, H.J., Teng, Z.D.: Pinning synchronization of weighted complex networks with variable delays and adaptive coupling weights. Nonlinear Dyn. **67**, 1373–1385 (2012)
13. Wu, Y.Q., Li, C.P., Yang, A.L., Song, L.J., Wu, Y.J.: Pinning adaptive anti-synchronization between two general complex dynamical networks with non-delayed and delayed coupling. Appl. Math. Comput. **218**, 7445–7452 (2012)
14. Wu, X.J., Lu, H.T.: Outer synchronization between two different fractional-order general complex dynamical networks. Chin. Phys. B **19**, 070511 (2010)
15. Du, H.Y.: Function projective synchronization in drive-response dynamical networks with non-identical nodes. Chaos Solitons Fractals **44**, 510–514 (2011)
16. Wu, X.J., Lu, H.T.: Generalized projective synchronization between two different general complex dynamical networks with delayed coupling. Phys. Lett. A **374**, 3932–3941 (2010)
17. Zheng, S., Dong, G., Bi, Q.: Impulsive synchronization of complex networks with non-delayed and delayed coupling. Phys. Lett. A **373**, 4255–4259 (2009)
18. Zhang, Q.J., Zhao, J.C.: Projective and lag synchronization between general complex networks via impulsive control. Nonlinear Dyn. **67**, 2519–2525 (2012)
19. Guo, W., Austin, F., Chen, S.: Global synchronization of nonlinearly coupled complex networks with non-delayed and delayed coupling. Commun. Nonlinear Sci. Numer. Simul. **15**, 1631–1639 (2010)
20. Li, C.P., Sun, W.G., Kurths, J.: Synchronization between two coupled complex networks. Phys. Rev. E **76**, 046204 (2007)
21. Liu, T., Zhao, J., Hill, D.J.: Synchronization of complex delayed dynamical networks with nonlinearly coupled nodes. Chaos Solitons Fractals **40**, 1506–1519 (2009)
22. Wu, X., Zheng, W., Zhou, J.: Generalized outer synchronization between complex dynamical networks. Chaos **19**, 013109 (2009)
23. Hu, C., Yu, J., Jiang, H., Teng, Z.: Synchronization of complex community networks with non-identical nodes and adaptive coupling strength. Phys. Lett. A **375**, 873–879 (2011)
24. Ji, D.H., Jeong, S.C., Park, J.H., Lee, S.M., Won, S.C.: Adaptive lag synchronization for uncertain complex dynamical network with delayed coupling. Appl. Math. Comput. **218**, 4872–4880 (2012)
25. Zheng, S.: Adaptive-impulsive projective synchronization of drive-response delayed complex dynamical networks with time-varying coupling. Nonlinear Dyn. **67**, 2621–2630 (2012)
26. Wu, X.J., Lu, H.T.: Generalized function projective (lag, anticipated and complete) synchronization between two different complex networks with non-identical nodes. Commun. Nonlinear Sci. Numer. Simul. **17**, 3005–3021 (2012)
27. Wang, J.L., Wu, H.N.: Local and global exponential output synchronization of complex delayed dynamical networks. Nonlinear Dyn. **67**, 497–504 (2012)
28. Gualberto, S.P.: Complete synchronization of strictly different chaotic systems. Am. J. Math. **2012**, 964179 (2012)
29. Wang, Z.L., Shi, X.R.: Anti-synchronization of Liu system and Lorenz system with known or unknown parameters. Nonlinear Dyn. **57**, 425–430 (2009)
30. Mahmoud, G., Mahmoud, E.: Phase and antiphase synchronization of two identical hyperchaotic complex nonlinear systems. Nonlinear Dyn. **61**, 141–152 (2010)
31. Guo, W.: Lag synchronization of complex networks via pinning control. Nonlinear Anal., Real World Appl. **12**, 2579–2585 (2011)
32. Rao, P.C., Wu, Z.Y., Liu, M.: Adaptive projective synchronization of dynamical networks with distributed time delays. Nonlinear Dyn. **67**, 1729–1736 (2012)
33. Dai, H., Jia, L.X., Hui, M., Si, G.Q.: A new three-dimensional chaotic system and its modified generalized projective synchronization. Chin. Phys. B **20**, 040507-10 (2011)
34. Jia, L.X., Dai, H., Hui, M.: A new four-dimensional hyperchaotic Chen system and its generalized synchronization. Chin. Phys. B **19**, 100501-11 (2010)
35. Chen, D.Y., Zhao, W.L., Ma, X.Y., Zhang, R.F.: Control and synchronization of chaos in RCL-shunted Josephson

junction with noise disturbance using only one controller term. Abstr. Appl. Anal. **2012**, 378457 (2012)

36. Yassen, M.T.: Controlling chaos and synchronization for new chaotic system using linear feedback control. Chaos Solitons Fractals **26**, 913–920 (2005)

37. Chen, D.Y., Shi, L., Chen, H.T., Ma, X.Y.: Analysis and control of a hyperchaotic system with only one nonlinear term. Nonlinear Dyn. **67**, 1745–1752 (2012)

38. Yang, L.X., He, W.S., Liu, X.J.: Synchronization between a fractional-order system and an integer order system. Comput. Math. Appl. **62**, 4708–4716 (2011)

39. Chen, D.Y., Zhang, R.F., Sprott, J.C., Chen, H.T., Ma, X.Y.: Synchronization between integer-order chaotic systems and a class of fractional-order chaotic systems via sliding mode control. Chaos **22**, 023130 (2012)